

Three Phase Lag Bioheat Transfer Model for Evaluating Heat Transfer by Hyperthermia Treatment in Tissue

Neha Sharma, Surjan Singh and Dinesh Kumar

Abstract— Hyperthermia occurs when the body takes in or out more heat than it can normally release. When treating hyperthermia, it's critical to determine the biological tissue's temperature profile. This article examines the simulation and mathematical modeling of the three-phase-lag bioheat transfer (TPLBHT) model underneath periodic boundary conditions. The central difference approach, which transforms the problem into ODEs of the initial value problem, and the Runge-Kutta (4, 5) scheme methodology to explain the initial value problem have been employed to conclude the mathematical study of the current TPLBHT problem. We took into consideration the metabolic heat source and blood circulation, both of which had experimental validation. The whole document is written in a non-dimensional form and is analyzed. The effects of various dimensionless parameters are explained thoroughly, like blood perfusion source, heat source, relaxation time, thermalization time, and other TPL parameters on dimensionless temperature.

Index Terms— Bioheat transfer, Blood Perfusion, Hyperthermia, Modelling, Runge-Kutta (4, 5).

ABBREVIATIONS

PBHT	Pennes bioheat transfer model
SPL	Single phase lag
DPL	Dual phase lag
DPLBHT	Dual phase lag bioheat transfer
TPL	Three phase lag
TPLBHT	Three phase lag bioheat transfer
FDM	Finite difference method
RKM	Runge Kutta method

DIMENSIONAL PARAMETERS

q	heat flux, W/m^2
x	space coordinate, m
t	time, s
k	thermal conductivity of tissue, $W/m^{\circ}C$
k^*	rate of thermal conductivity of living tissue
T	temperature of tissue, $^{\circ}C$
τ_q	phase lag because of heat flux, s
τ_T	phase lag because of temperature gradient, s
τ_v	phase lag because of thermal displacement, s
ρ	density of tissue, kg/m^3

c	specific heat of tissue, $J/kg^{\circ}C$
w_b	rate of blood circulation, s^{-1}
ρ_b	density of blood, kg/m^{-3}
c_b	specific heat of blood, $J/kg^{\circ}C$
T_b	arterial blood temperature, $^{\circ}C$
ω	periodicity, s^{-1}
Q_{mo}	reference intensity of metabolism, w/m^3
L	range of tissue, m
T_w	wall thermal of outermost boundary, $^{\circ}C$

NON-DIMENSIONAL PARAMETERS

y	Non-dimensional space coordinate
ξ	Non-dimensional time
F_{oq}	Non-dimensional phase lag because of heat flux
F_{oT}	Phase lag because of temperature gradient
F_{ov}	Phase lag because of thermal displacement
θ	Temperature of local tissue
θ_b	Temperature of arterial blood
γ	Non-dimensional associated metabolic constant
α	Non-dimensional associated blood perfusion constant
ω	Non-dimensional periodicity
θ_w	Non-dimensional wall temperature at boundary
H_f	Non-dimensional blood perfusion coefficient
H_m	Non-dimensional metabolic heat.source coefficient
K_T	Non-dimensional thermal conductivity

I. INTRODUCTION

Hyperthermia, which is a process that elevates temperature on a specific part of the body or whole body for a definite period of time. It can be performed in three categories: localized, regional, and whole-body hyperthermia.

Due to several problems related to different types of cancer therapy, heating methods have been developed. The word hyperthermia usually refers to either an abnormally high fever or the therapeutics of the condition by the induction of fever. Hyperthermia has a different effect determined by the temperature and duration of exposure. The first research publication on hyperthermia was in 1886. The article discussed the challenges and possibilities of hyperthermia, which will happen in the future. The mathematical modelling of bioheat transfer is given by the PBHT model [1]. This model is derived from the heat conduction Fourier law, presumes that the thermal signal has an infinite velocity as

$$q(x, t) = -k\nabla T(x, t), \quad (1)$$

where $q(x, t)$, k , T stands for the heat flux, thermal conductivity, and thermal tissue, respectively. When the heat moves throughout tissue and blood, then it takes a finite gap, i.e. the

Manuscript received 30 November, 2024; revised September 22, 2024.

Neha Sharma is a PhD candidate of Eternal University, Baru Sahib, 173101, India (email: nehasharma07111993@gmail.com).

Surjan.Singh is an Associate professor of Eternal University, Baru Sahib, 173101, India. (Corresponding author, phone: 8580806659, email: surjan.singhbhu@gmail.com).

Dinesh Kumar is an Assistant Professor of Mathematics, Government Polytechnic College, Nawada, Bihar, 805122, India (email:dineshaukumar@gmail.com).

lagging behaviour exists. Cattaneo [2] and Vernotte [3] individually suggested a relaxation time τ_q that is because of heat flux to solve the inconsistency caused by the infinite gap velocity of the thermal signal, referred to as SPL constitutive relation as:

$$q(x, t + \tau_q) = -k \nabla T(x, t), \quad (2)$$

The combination of SPL relation and energy balance equation shows a bioheat model of thermal wave.

The SPL model was further studied by Tzou [4] and gives a phase lag time that occurs because of the temperature gradient τ_T and is called DPL constitutive relation as:

$$q(x, t + \tau_q) = -k \nabla T(x, t + \tau_T), \quad (3)$$

When the DPL model is integrate with energy balance equation, then it becomes the DPLBHT model. Several researchers [5-13] explained the third phase lag τ_v and combined with the DPL constitutive relation with temperature displacement, known as the TPL constitutive relation, i.e.

$$q(x, t + \tau_q) = -[k \nabla T(x, t + \tau_T) + k^* \nabla v(x, t + \tau_v)], \quad (4)$$

where $v(x, t)$ is thermal displacement and $\frac{\partial v(x, t)}{\partial t} = T(x, t)$, k^* stands for thermal conductivity rate of tissue.

We used the expansion of Taylor's series of the TPL model up to first order at time t in the present problem as:

$$\left(1 + \tau_q \frac{\partial}{\partial t}\right) q(x, t) = -\left[\tau_v^* \nabla T(x, t) + k \tau_T \frac{\partial}{\partial t} \nabla T(x, t) + k^* \nabla v(x, t)\right], \quad (5)$$

Where $\tau_v^* = (k + k^* \tau_v)$

Moroz [14] reviewed the four sub-classes, which are arterial blockage, direct injection, intracellular, and interstitial insert hyperthermia, in terms of clinical results, advantages, disadvantages, and current status in hyperthermia treatment.

Askarizadeh [15] used the DPLBHT model for the treatment of the transient transfer of heat problems in epidermis tissues through periodic heat flux. Comparisons of previous studies results and analytical results by taking Jacobi elliptic functions are shown. The results of thermal conductivity, metabolic heat, perfusion of blood, and the coefficient of transfer of heat in biological tissues on the temperature profile are numerically shown by Kengnea [16]. Ahmadikia [17] gave solutions of hyperbolic and parabolic bioheat transfer models under pulse heat flux, periodic, and constant BCs. Using the Laplace transform approach, the problem is analytically described by taking into consideration finite and semi-infinite domains.

Yuan [18] investigated the porous model on hyperthermia therapy of the heat transformation coefficient in tissue and blood and applied the FDM for solving the PBHT equation. Salloum [19] determined the highest heating patterns in the instigated tumour model with nanoparticle injections of irregular geometries in hyperthermia. Ghazanfarian [20] discretized the non-linear PBHT equation and DPL model by using a procedure of mesh-free smoothed particle hydrodynamics method.

Gupta [21] described the method of transfer of heat with blood perfusion having different BCs and coordinate systems by radiations of electromagnet using the Adomian decomposition method. Khanafer [22] mathematically studied the flow of pulsatile laminar and rising temperature protocol on thermal profile in hyperthermia treatment. They validated their numerical results by comparing them with previous studies. The response of heating and thermal dose of tissue underneath non-equilibrium conditions for hyperthermia therapy has been

investigated by Yuan [23]. Jalali [24] introduced the method to control the temperature profile across the tissue, which can be derived by proper handling of functional variables in hyperthermia. A finite volume scheme is used to evaluate the problem. Jiwari [25] offered a numerical method that depends on the polynomial of the differential quadrature example for finding the solutions of the 2D Sine-Gordon equation under second-kind BCs. Song [26] studied the responses of hyperthermia on the blood flow. Choudhuri [27] obtained a TPL model by an extension of models of thermoelastic explained by Tzou, Green-Naghdi, and Lord-Shulman.

The thermal behaviour of the DPL model of transfer of bioheat in living tissue during thermal therapy is reviewed by Kumar [28-33]. The FEWG, FDM, and R-K (4, 5) methods are used to evaluate the non-linear model, and the outcomes are compared to the exact answer found by Laplace and its inversion approach. In hyperthermia treatment, Kumar [34] explained by studying the DPL model of transfer of bioheat by using a Gaussian distribution source underneath generalized BC by using the finite element wavelet Galerkin scheme. Liu [35] analyzed the behaviour of temperature during hyperthermia treatment in biological tissues within the DPL model.

Reis [36] adopted the PBHT equation for the thermal tumour ablation of magnetic nanoparticles, to get the good hyperthermia condition by using the explicit finite difference method. Sharma [37] calculated the mathematical- based modelling and its simulation of bioheat transfer underneath the Dirichlet BC with complex nonlinear DPLBHT for the temperature profile in tissues of infected cells during treatment of hyperthermia. Bagaria [38] considered the tissue model taking a spherical region for magnetic fluid hyperthermia treatment.

In this article, we explained the mathematical modelling and simulation of the TPLBHT model for hyperthermia treatment. Temperature-dependent terms that have been verified through experimental are the metabolic heat and blood perfusion terms. The whole work has been resolved and composed in a non-dimensional format. The hybrid approach is used to address the present problem. Using central FDM, the third order partial differential equation problem is transformed into ODEs. Again converting third order ODEs into first order differential equations and solving with the R-K (4, 5) method. The parameters impact used in the TPLBHT model are shown in Figures. The formulation of the hybrid method is shown in the following sections.

II. FORMATION OF THE PROBLEM

In this research paper, we considered a 1-D inner structure of length L with introductory temperature T_o in skin tissue. The inner boundary of skin tissue ($x = 0$) and exterior surface of skin tissue ($x = L$) are insulated is presented by Figure 1

$$T(0, t) = T_w$$

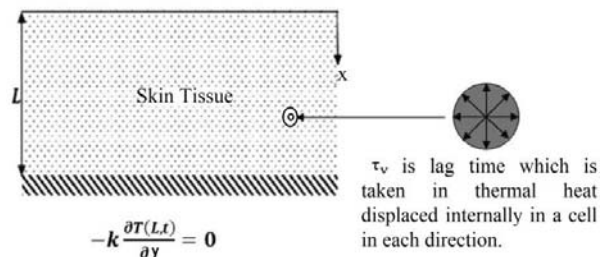


Fig 1. Schematic representation of skin tissue in one dimension.

The 1-D energy balance equation is generally conducted by PBHT equation [1] is

$$\rho c \frac{\partial T(x,t)}{\partial t} = -\nabla q(x,t) + q_b + q_m, \quad (6)$$

where ρ is the density of tissue; c is the specific heat of tissue; t is time $q(x,t)$ is the heat flux; q_b and q_m are the heat of blood perfusion and metabolic source respectively.

Metabolic heat source is the temperature depended which is the source of local tissue temperature, given as: [6, 39]

$$q_m = q_{mo} \times 2^{\beta \left(\frac{T-T_0}{10} \right)} \quad (7)$$

where q_{mo} is the heat source reference term and β is the associated metabolic constant.

The blood perfusion source is given as: [32, 40]

$$q_b = w_b(T) \rho_b c_b (T_b - T) \quad (8)$$

where

$$w_b(T) = w_{bo} \times e^{\alpha \left(\frac{T-T_0}{10} \right)} \quad (9)$$

where ρ_b , c_b , $w_b(T)$ stands for the density, specific heat of blood and blood perfusion rate coefficient respectively. T_b is blood temperature and α is the associated blood perfusion constant.

By using (5) - (9), eliminating $q(x,t)$ which gives:

$$\tau_q \rho c \frac{\partial^3 T(x,t)}{\partial t^3} + \rho c \frac{\partial^2 T(x,t)}{\partial t^2} - \tau_q \frac{\partial^2 q_b}{\partial t^2} - \tau_q \frac{\partial^2 q_m}{\partial t^2} - \tau_q \frac{\partial q_b}{\partial t} - \tau_q \frac{\partial q_m}{\partial t} = \left[k^* + \tau_v^* \frac{\partial}{\partial t} + k \tau_T \right] \nabla^2 T(x,t). \quad (10)$$

Where $\tau_v^* = (k + k^* \tau_v)$

Subject to initial conditions

$$T(x,0) = T_0, \quad \frac{\partial T(x,0)}{\partial t} = 0, \quad \frac{\partial^2 T(x,0)}{\partial t^2} = 0. \quad (11)$$

Considering the periodic boundary condition as fluctuating temperature specified by Kumar [30] and Singh [41] as:

$$T(L,t) = T_w + A \cos(\omega t), \quad (12)$$

Inner boundary is insulated, therefore the heat flux at boundary is zero, i.e.,

$$\frac{\partial T(0,t)}{\partial x} = 0. \quad (13)$$

III. CONCLUSION OF THE PROBLEM

To convert the equation into dimensionless form and reduce some parameters in the equation so that it is easy to solve, we define the dimensionless variables, which are as follows:

$$y = \frac{x}{L}, \quad \xi = \frac{kt}{\rho c L^2}, F_{oq} = \frac{k \tau_q}{\rho c L^2}, F_{oT} = \frac{k \tau_T}{\rho c L^2}, F_{ov} = \frac{k \tau_v}{\rho c L^2}, \\ \theta = \frac{T - T_0}{T_0}, H_m = \frac{q_{mo} L^2}{k T_0}, H_f = \sqrt{\frac{w_b c_b \rho_b}{k}} L, K_T = \sqrt{\frac{k^* \rho c}{k}} L, \gamma = 0.1 \times T_0 \times \beta.$$

By using dimensionless parameters in (10) - (13), the equations become

$$F_{oq} \frac{\partial^3 \theta(y,\xi)}{\partial \xi^3} = -\{1 - F_{oq} \gamma H_m \log(2) 2^{\gamma \theta} - F_{oq} H_f^2 e^{\alpha \theta} (\alpha(\theta_b - \theta) - 1)\} \frac{\partial^2 \theta(y,\xi)}{\partial \xi^2} + \\ (H_f^2 e^{\alpha \theta} (\alpha(\theta_b - \theta) - 1) + \gamma H_m \log(2) 2^{\gamma \theta}) \frac{\partial \theta(y,\xi)}{\partial \xi} - \\ F_{oq} H_m \gamma^2 (\log(2))^2 2^{\gamma \theta} + \left(\frac{\partial \theta(y,\xi)}{\partial \xi} \right)^2 + K_T^2 \frac{\partial^2 \theta(y,\xi)}{\partial y^2} + \\ F_{oq} H_f^2 e^{\alpha \theta} \alpha (\alpha(\theta_b - \theta) - 2) + F_{ov}^* \frac{\partial^3 \theta(y,\xi)}{\partial \xi \partial y^2} + F_{oT} \frac{\partial^4 \theta(y,\xi)}{\partial \xi^2 \partial y^2}. \quad (14)$$

Where $F_{ov}^* = 1 + K_T^2 F_{ov}$

Subject to initial conditions

$$\theta(y,0) = 0, \quad \frac{\partial \theta(y,\xi)}{\partial \xi} = 0, \quad \frac{\partial^2 \theta(y,\xi)}{\partial \xi^2} = 0. \quad (15)$$

Boundary condition

$$\theta(1,\xi) = \theta_w + A \cos(\omega \xi), \quad (16)$$

and symmetric condition

$$\frac{\partial \theta(0,\xi)}{\partial \xi} = 0. \quad (17)$$

IV. HYBRID.NUMERICAL.METHOD

The hybrid method is implemented to resolve the problem numerically. This method is a combination of two different methods. The first method in which (14) is discretized by FDM by using the central difference method, given by many researchers [32, 42, 43]. After discretization, our problem is turned into a third order non-linear ODEs with initial conditions. Again converting third order ODEs into first-order non-linear ordinary differential equations [44]. For the results of the problem, the second method, which is the R-K (4, 5) [25, 45, 46] scheme, is applied. The whole procedure of the hybrid scheme is explained in the next sub-section.

SPATIAL DISCRETIZATION SCHEME

The domain of space coordinate [0,1] is discretized into $l + 1$ sub intervals of equivalent length h by taking $y_{i+1} = y_i + 1$ i.e, $0 = y_0 < y_1 < y_2 < y_3 < \dots < y_i < \dots < y_l < y_{l+1} = 1$. By applying central finite difference formula, the second order derivative is written as,

$$\frac{\partial^2 \theta(y,\xi)}{\partial y^2} = \frac{\theta_{i+1}(\xi) - 2\theta_i(\xi) + \theta_{i-1}(\xi)}{h^2}, \quad 1 \leq i \leq l, \quad (18)$$

Then the (14) - (17) converted by the above equation as

$$F_{oq} \frac{d^3 \theta_1}{d\xi^3} = -\{1 - F_{oq} \gamma H_m \log(2) 2^{\gamma \theta_1} - F_{oq} H_f^2 e^{\alpha \theta_1} (\alpha(\theta_b - \theta_1) - 1)\} \frac{d^2 \theta_1}{d\xi^2} + \\ (H_f^2 e^{\alpha \theta_1} (\alpha(\theta_b - \theta_1) - 1) + \gamma H_m \log(2) 2^{\gamma \theta_1}) \frac{d\theta_1}{d\xi} - \\ \{F_{oq} H_m \gamma^2 (\log(2))^2 2^{\gamma \theta_1} - F_{oq} H_f^2 e^{\alpha \theta_1} \alpha (\alpha(\theta_b - \theta_1) - 2)\} \\ \left(\frac{d\theta_1}{d\xi} \right)^2 + K_T^2 \frac{d^2 \theta_1}{dy^2} + F_{ov}^* \frac{d^3 \theta_1}{d\xi dy^2} + F_{oT} \frac{d^4 \theta_1}{d\xi^2 dy^2}, \quad (19)$$

$$F_{oq} \frac{d^3 \theta_i}{d\xi^3} = -\{1 - F_{oq} \gamma H_m \log(2) 2^{\gamma \theta_i} - F_{oq} H_f^2 e^{\alpha \theta_i} (\alpha(\theta_b - \theta_i) - 1)\} \frac{d^2 \theta_i}{d\xi^2} + \\ (H_f^2 e^{\alpha \theta_i} (\alpha(\theta_b - \theta_i) - 1) + \gamma H_m \log(2) 2^{\gamma \theta_i}) \frac{d\theta_i}{d\xi} - \\ \{F_{oq} H_m \gamma^2 (\log(2))^2 2^{\gamma \theta_i} - F_{oq} H_f^2 e^{\alpha \theta_i} \alpha (\alpha(\theta_b - \theta_i) - 2)\} \\ \left(\frac{d\theta_i}{d\xi} \right)^2 + K_T^2 \frac{d^2 \theta_i}{dy^2} + F_{ov}^* \frac{d^3 \theta_i}{d\xi dy^2} + F_{oT} \frac{d^4 \theta_i}{d\xi^2 dy^2}, \quad (20)$$

$$F_{oq} \frac{d^3 \theta_n}{d\xi^3} = -\{1 - F_{oq} \gamma H_m \log(2) 2^{\gamma \theta_n} - F_{oq} H_f^2 e^{\alpha \theta_n} (\alpha(\theta_b - \theta_n) - 1)\} \frac{d^2 \theta_n}{d\xi^2} + \\ (H_f^2 e^{\alpha \theta_n} (\alpha(\theta_b - \theta_n) - 1) + \gamma H_m \log(2) 2^{\gamma \theta_n}) \frac{d\theta_n}{d\xi} - \\ \{F_{oq} H_m \gamma^2 (\log(2))^2 2^{\gamma \theta_n} - F_{oq} H_f^2 e^{\alpha \theta_n} \alpha (\alpha(\theta_b - \theta_n) - 2)\} \\ \left(\frac{d\theta_n}{d\xi} \right)^2 + K_T^2 \frac{d^2 \theta_n}{dy^2} + F_{ov}^* \frac{d^3 \theta_n}{d\xi dy^2} + F_{oT} \frac{d^4 \theta_n}{d\xi^2 dy^2}, \quad (21)$$

Subject to initial conditions $\theta(y,0) = 0, \frac{d\theta(y,\xi)}{d\xi} = 0, \frac{d^2 \theta(y,\xi)}{d\xi^2} = 0. \quad (22)$

RUNGE - KUTTA (4, 5) SCHEME

Lets suppose that [44]

$$\frac{d}{dz} (F_{oq} \frac{d^2\theta}{dz^2}) = \frac{d\psi}{dz} \frac{d^2\theta}{dz^2} = \frac{\psi}{F_{oq}} \frac{d}{dz} (\frac{d\theta}{dz}) = \frac{\psi}{F_{oq}} \frac{d\theta}{dz} = \frac{\varphi}{F_{oq}}$$

(23)

By using (23), then (19) - (22) can be reduced in

$$\psi'_1 = -1 + F_{oq}\gamma H_m \log(2)2^{\gamma\theta_1} + F_{oq}H_f^2 e^{\alpha\theta_1}(\alpha(\theta_b - \theta_1) - 1) + \gamma H_m \log(2)2^{\gamma\theta_1} \frac{\varphi_1}{F_{oq}} - \{F_{oq}H_m\gamma^2(\log(2))^2 2^{\gamma\theta_1} - F_{oq}H_f^2 e^{\alpha\theta_1}\alpha(\alpha(\theta_b - \theta_1) - 2)\} \frac{\varphi_1^2}{F_{oq}} + \frac{K_T^2}{21h^2}(-29\theta_1 + 38\theta_2 - 9\theta_3) + \frac{F_{ov}^*}{21F_{oq}h^2}(-29\varphi_1 + 38\varphi_2 - 9\varphi_3) + \frac{F_{oT}}{21F_{oq}h^2}(-29\psi_1 + 38\psi_2 - 9\psi_3), \quad (24)$$

$$\psi'_i = -1 + F_{oq}\gamma H_m \log(2)2^{\gamma\theta_i} + F_{oq}H_f^2 e^{\alpha\theta_i}(\alpha(\theta_b - \theta_i) - 1) + \gamma H_m \log(2)2^{\gamma\theta_i} \frac{\varphi_i}{F_{oq}} - \{F_{oq}H_m\gamma^2(\log(2))^2 2^{\gamma\theta_i} - F_{oq}H_f^2 e^{\alpha\theta_i}\alpha(\alpha(\theta_b - \theta_i) - 2)\} \frac{\varphi_i^2}{F_{oq}} + \frac{K_T^2}{21h^2}(\theta_{i+1} + \theta_i + \theta_{i-1}) + \frac{F_{ov}^*}{21oqh^2}(\varphi_{i+1} + \varphi_i + \varphi_{i-1}) + \frac{F_{oT}}{21F_{oq}h^2}(\psi_{i+1} + \psi_i + \psi_{i-1}), \quad 1 \leq i \leq l, \quad (25)$$

$$\psi'_n = -1 + F_{oq}\gamma H_m \log(2)2^{\gamma\theta_n} + F_{oq}H_f^2 e^{\alpha\theta_n}(\alpha(\theta_b - \theta_n) - 1) + \gamma H_m \log(2)2^{\gamma\theta_n} \frac{\varphi_n}{F_{oq}} - \{F_{oq}H_m\gamma^2(\log(2))^2 2^{\gamma\theta_n} - F_{oq}H_f^2 e^{\alpha\theta_n}\alpha(\alpha(\theta_b - \theta_n) - 2)\} \frac{\varphi_n^2}{F_{oq}} + \frac{K_T^2}{21h^2}(\theta_w + A \cos(\omega\xi) + \theta_n + \theta_{n-1}) + \frac{F_{ov}^*}{21oqh^2}(-A\omega \sin(\omega\xi) + \varphi_n + \varphi_{n-1}) + \frac{F_{oT}}{21F_{oq}h^2}(-A\omega^2 \cos(\omega\xi) + \psi_n + \psi_{n-1}), \quad (26)$$

Subject to initial conditions
 $\theta(y, 0) = 0, \quad \varphi(y, 0) = 0, \quad \psi(y, 0) = 0. \quad (27)$

V. RESULT AND DISCUSSIONS

When the outermost region was kept at a temperature which is constant, the thermal distribution in the body was identified using the non-linear TPLBHT model in the present mathematical technique. The perfusion term and metabolic term in the model are temperature-dependent and have been verified experimentally. We explained the parameters, which are distinct from reference values. Graphical representations of results are shown in Figures (2 - 11). For the computation of a non-dimensional temperature profile in a finite domain in biological skin tissue, the particular reference value of non-dimensional terms is as follows:

Table 1. Physical properties of biological tissue.

Specifications	Dimensions	Numeric Quantities	Reference s
Thermal Conductivity	$W/m^{\circ}C$	0.5	[34]
Wall temperature	$^{\circ}C$	39.5	[34]
Initial temperature	$^{\circ}C$	37	[34]
Specific heat	$J/kg^{\circ}C$	4000	[34]
Density	kg/m^3	1000	[47]
Thickness	m	0.05	[47]
Blood's density	kg/m^3	1060	[47]
Specific heat	$J/kg^{\circ}C$	3860	[47]

Blood temperature	$^{\circ}C$	37	[47]
Lag time because of heat flux	s	600	[28]
Lag time because of temperature gradient	s	300	[28]
Lag time because of thermal displacement	s	100	[6]
Associated metabolic constant	$^{\circ}C^{-1}$	2.15	[32]
Initial blood perfusion coefficient	-	2.15	[32]
Blood perfusion rate	w/m^3	2.14×10^{-2}	[40]
Metabolic generation of heat	w/m^3	50.65	[39]
Thermal conductivity rate	$W/m^{\circ}C/s$	6.25×10^{-5}	[6]

Hyperthermia is used for the treatment depending on the different duration and temperature level, such as 41 – 45°C for 15 – 60 min. The arithmetic model of heating the skin tissues is obtained from the standard Fourier hypothesis of heat conduction. When the non-linear TPLBHT model is identified with verified metabolic processes and human blood perfusion, computational results give an accurate temperature profile in tissue. For the calculation of the temperature in tissue, this research will be beneficial for the therapist for precise treatment.

The hybrid numeric method, which is depends on the FDM and the R-K (4, 5) method which refers to the FERK (4, 5) scheme, is employed for the numerical solution of the non-linear the TPLBHT model for the tissue.

The result of dimensionless lagging time because of heat flux F_{oq} is observed in Figure 2 with respect to non-dimensional temperature and time. In which we notice that as the rate of F_{oq} increases, the thermal profile increases. In Figure 3, the impact of non-dimensional lagging time because of temperature gradient F_{oT} is shown. It has been concluded that thermal wave of temperature profile rises as value of F_{oT} decreases. From Figure 4, it has been noticed that as increasing the values of phase lag time, which is because of thermal displacement F_{ov} , the temperature distribution wave increases.

Therefore, F_{oq}, F_{oT}, F_{ov} affects on temperature profile concluded from Figures 2-4. The behavior of periodicity on temperature profile and time is shown in Figure 5. It shows that the amplitude of temperature is highest on $\omega = 0$ and falls as the value of ω rises. Blood perfusion and metabolic heat have important impact on heat transfer in tissue. Blood perfusion manages to transfer the oxygen, nutrients, and waste products.

In Figure 6, the effect of dimensionless blood perfusion source H_f is shown with respect to non-dimensional temperature and time. We determined that the temperature distribution decreases as increasing the blood perfusion H_f term. Similarly, metabolic heat generation is the heat released by physical activities. Figure 7 shows the effect of a dimensionless metabolic heat source H_m with temperature and time.

It has been concluded that temperature is approximately same for $H_m = 2.2973e - 00$ and $H_m = 2.2973e - 01$, and it rises for value of $H_m = 2.2973e - 05$.

In Figure 8, the impact of amplitude A is obtained with respect to non-dimensional temperature and time. It described that thermal wave rises as the value of A increases. In Figure 9, the wave of temperature profile rises while increasing the value of the dimensionless associated metabolic constant γ . The results of blood perfusion constant α with respect to non-dimensional temperature and time are presented in Figure 10. It has been concluded that as increasing the value of α the temperature profile decreases. Figure 11 introduces the effect of K_T with respect to non-dimensional temperature and time, which shows that the wave of temperature profile increases as increasing the value of K_T .

VI. CONCLUSION

The mathematical modelling and simulation of the non-linear TPLBHT model is solved by using periodic boundary conditions. The observations from the present problem are concluded as follows:

- The hybrid methodology was used for the results of the non-linear TPLBHT model, which gives high accuracy with lesser computation.
- For the hyperthermia, the effect of temperature profiles is shown on the various values of the parameters.
- When the value of F_{oq} increases with respect to non-dimensional temperature and time, then the temperature profile decreases, while as F_{oT} and F_{ov} increases, the temperature distribution decreases.
- As increasing the value of H_m the temperature wave decreases while reduces the value of H_f , the thermal wave of the temperature profile decreases.
- It is achieved that as increasing the value of γ and α , the thermal wave of temperature profile increases and decreases, respectively.
- The value of K_T and A increases with respect to non-dimensional time, then thermal distribution increases while the value of ω decreases, the temperature profile increases.

Based on all these observations, we observed that the presented non-linear TPLBHT model played an important role in the hyperthermia treatment of malignant cells.

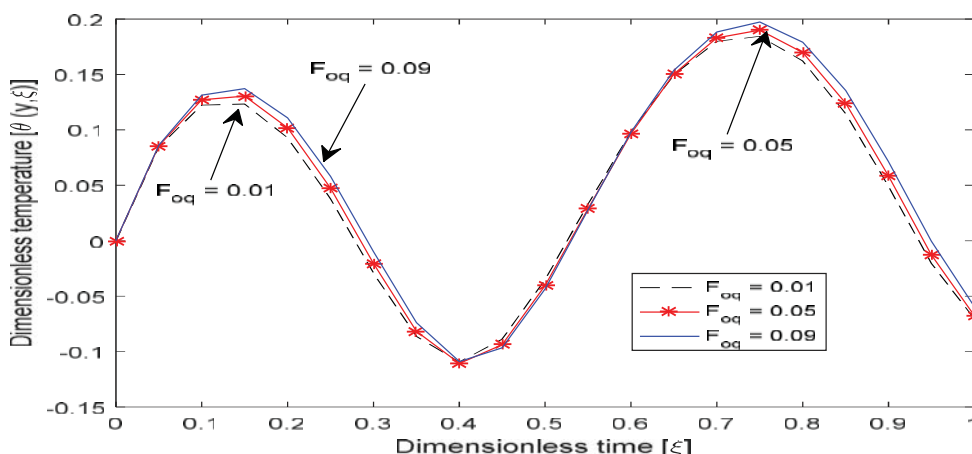


Fig 2. Comparison of the dimensionless thermal profile with time for the dimensionless phase lag time because of heat flux parameter.

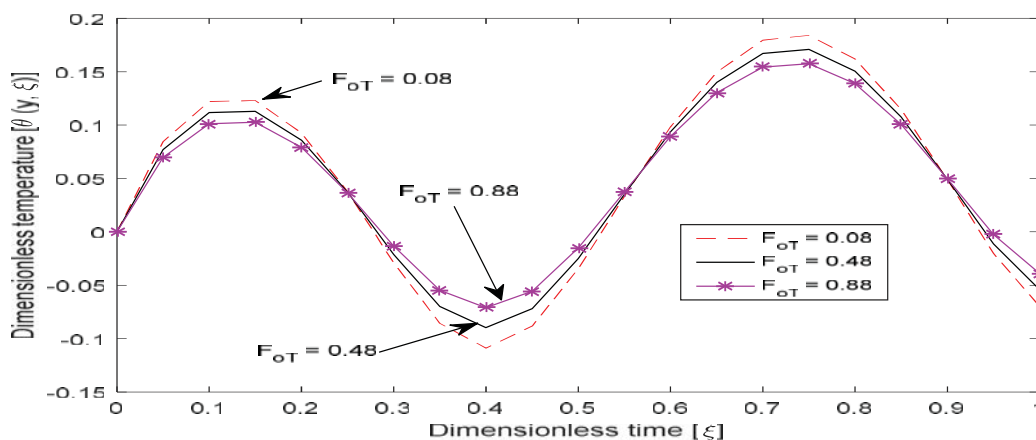


Fig 3. Comparison of the dimensionless thermal profile distribution with time for dimensionless phase lag because of thermal gradient.

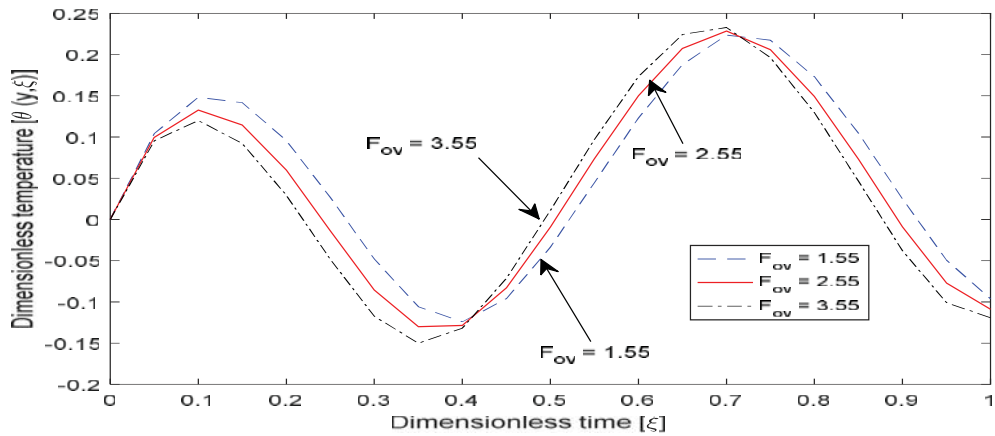


Fig 4. Comparison of the dimensionless thermal profile distribution with time for different values of the phase lag because of thermal displacement.

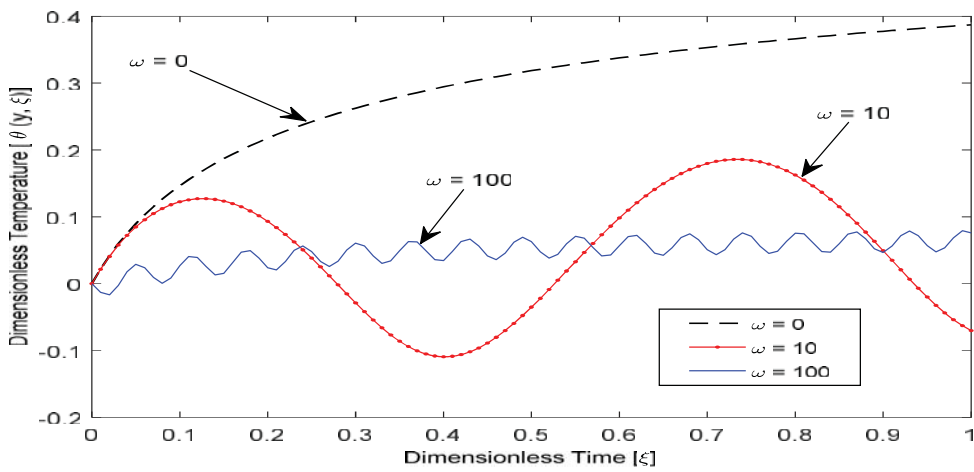


Fig 5. Impact of ω on dimensionless thermal distribution in tissue with respect to dimensionless time.

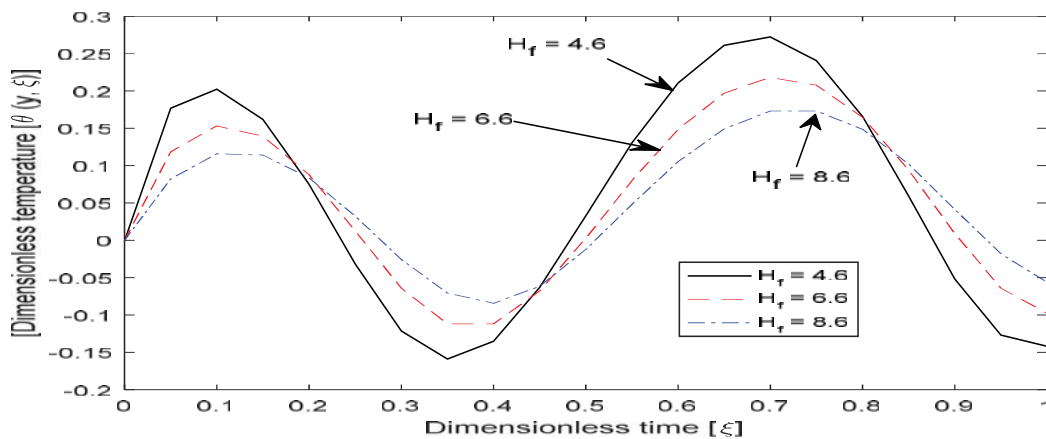


Fig 6. Representation of the dimensionless thermal profile distribution with time for different values of the blood perfusion source.

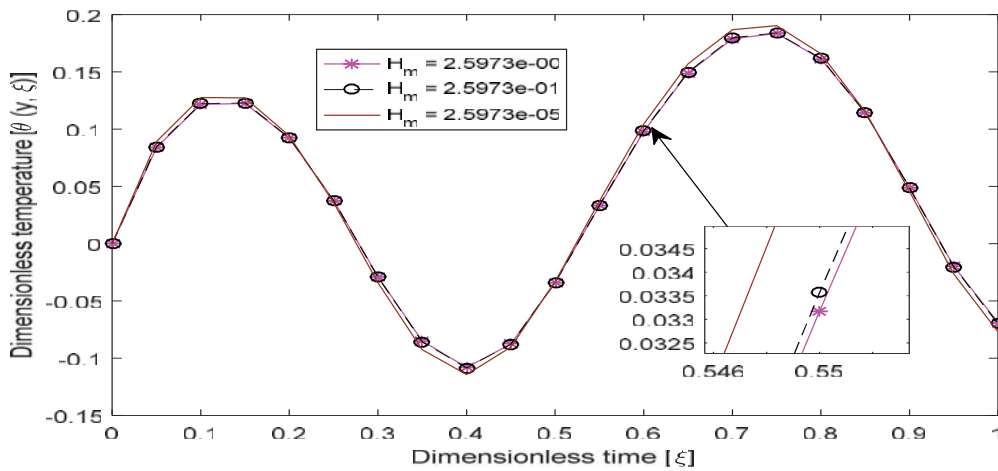


Fig 7. Shows the comparison of dimensionless thermal distribution with time for various values of the dimensionless metabolic heat source.

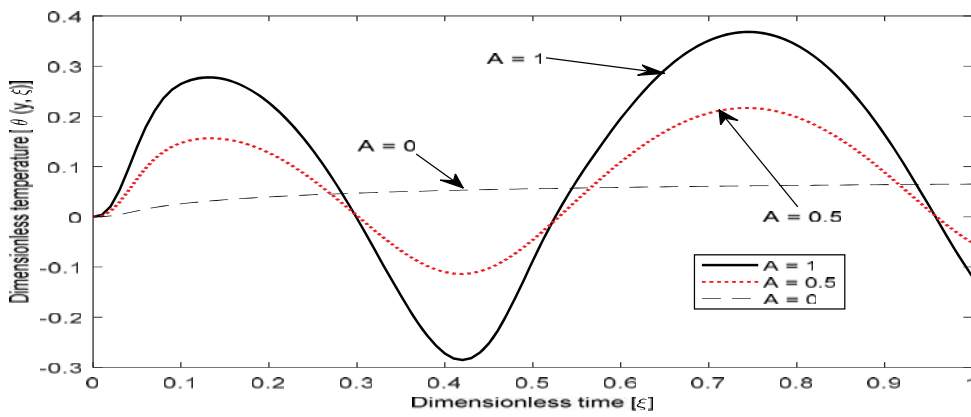


Fig 8. Impact of A on dimensionless thermal profile in tissue with respect to dimensionless time.

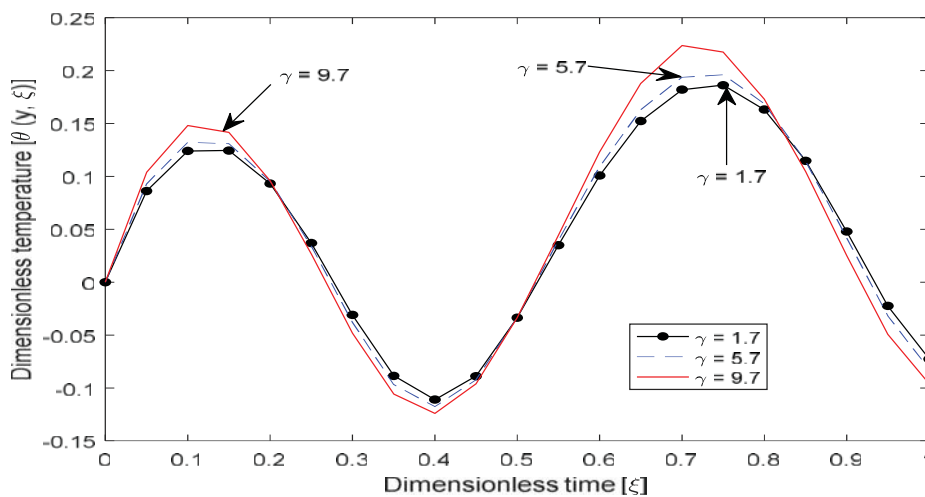


Fig 9. Comparison of the dimensionless thermal profile with time for various values of the dimensionless blood perfusion constant.

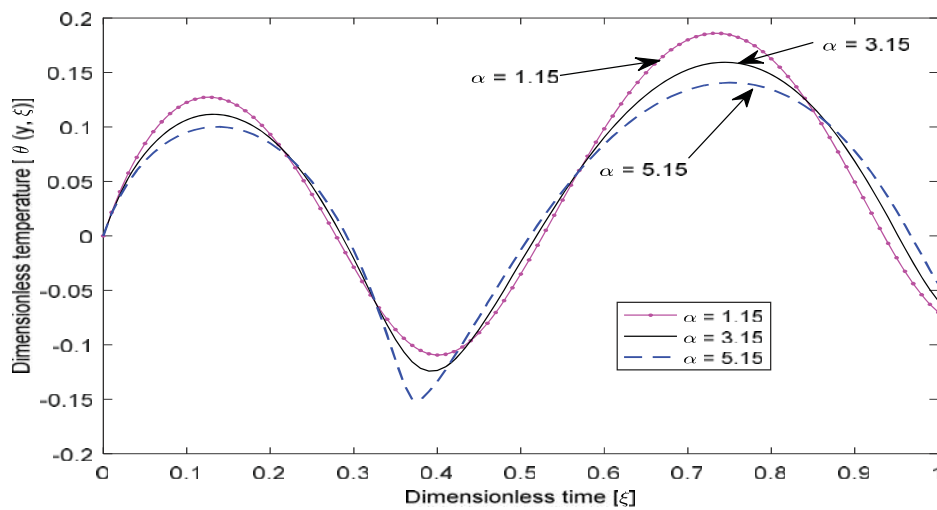


Fig 10. Representation of the dimensionless thermal profile with time for various values of the blood perfusion constant.

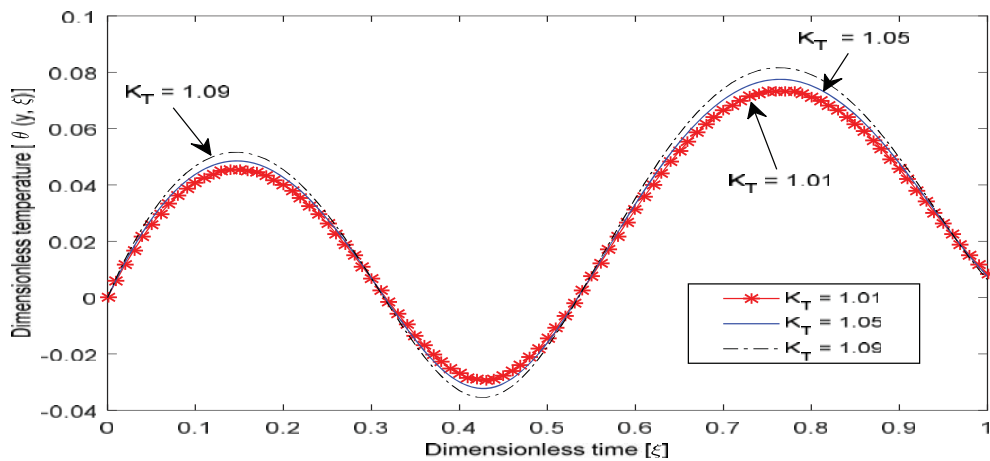


Fig 11. Impact of K_T on dimensionless temperature profile in tissue with respect to dimensionless time.

REFERENCES

[1] H. H. Pennes, "Analysis of tissue and arterial blood temperatures in the resting human forearm," *Journal of applied physiology*, vol 1, pp. 93-122, 1948.

[2] C. Cattaneo, "Sur une forme de l'equation de la chaleur eliminant la paradoxe d'une propagation instantanee," *Compt. Rendu*, vol 247, pp. 431-433, 1958.

[3] P. Vernotte, "Les paradoxes de la theorie continue de l'equation de la chaleur," *Comptes rendus*, vol 246, p. 3154, 1958.

[4] D. Y. Tzou, *Macro-to microscale heat transfer: the lagging behavior*: John Wiley & Sons, 2014.

[5] M. Ferreira and J. I. Yanagihara, "A transient three-dimensional heat transfer model of the human body," *International Communications in heat and mass transfer*, vol 36, pp. 718-724, 2009.

[6] D. Kumar and K. Rai, "Three-phase-lag bioheat transfer model and its validation with experimental data," *Mechanics Based Design of Structures and Machines*, vol 50, pp. 2493-2507, 2022.

[7] R. Quintanilla and R. Racke, "A note on stability in three-phase-lag heat conduction," *International Journal of Heat and Mass Transfer*, vol 51, pp. 24-29, 2008.

[8] R. Tiwari and R. Kumar, "Analysis of plane wave propagation under the purview of three phase lag theory of thermoelasticity with non-local effect," *European Journal of Mechanics-A/Solids*, vol 88, p. 104235, 2021.

[9] Q. Zhang, Y. Sun, and J. Yang, "Thermoelastic responses of biological tissue under thermal shock based on three phase lag model," *Case Studies in Thermal Engineering*, vol 28, p. 101376, 2021.

[10] R. Kumar, A. K. Vashishth, and S. Ghangas, "Phase-lag effects in skin tissue during transient heating," *International Journal of Applied Mechanics and Engineering*, vol 24, pp. 603-623, 2019.

[11] R. Tiwari and J. Misra, "Magneto-thermoelastic excitation induced by a thermal shock: a study under the purview of three phase lag theory," *Waves in Random and Complex Media*, vol 32, pp. 797-818, 2022.

[12] S. Chiriță, C. D'Apice, and V. Zampoli, "The time differential three-phase-lag heat conduction model: Thermodynamic compatibility and continuous dependence," *International Journal of Heat and Mass Transfer*, vol 102, pp. 226-232, 2016.

[13] R. Kumar, S. Devi, and S. Abo-Dahab, "Propagation of Rayleigh waves in modified couple stress generalized thermoelastic with a three-phase-lag model," *Waves in random and complex media*, vol 31, pp. 359-371, 2021.

[14] P. Moroz, S. Jones, and B. Gray, "Magnetically mediated hyperthermia: current status and future directions," *International Journal of Hyperthermia*, vol 18, pp. 267-284, 2002.

[15] H. Askarizadeh and H. Ahmadikia, "Analytical analysis of the dual-phase-lag model of bioheat transfer equation during

- transient heating of skin tissue," *Heat and Mass Transfer*, vol 50, pp. 1673-1684, 2014.
- [16] E. Kengne, A. Lakhssassi, and R. Vaillancourt, "Temperature distributions for regional hypothermia based on nonlinear bioheat equation of penne's type: dermis and subcutaneous tissues," 2012.
- [17] H. Ahmadikia, R. Fazlali, and A. Moradi, "Analytical solution of the parabolic and hyperbolic heat transfer equations with constant and transient heat flux conditions on skin tissue," *International communications in heat and mass transfer*, vol 39, pp. 121-130, 2012.
- [18] P. Yuan, "Numerical analysis of an equivalent heat transfer coefficient in a porous model for simulating a biological tissue in a hyperthermia therapy," *International Journal of Heat and Mass Transfer*, vol 52, pp. 1734-1740, 2009.
- [19] M. Salloum, R. Ma, and L. Zhu, "Enhancement in treatment planning for magnetic nanoparticle hyperthermia: optimization of the heat absorption pattern," *International Journal of Hyperthermia*, vol 25, pp. 309-321, 2009.
- [20] J. Ghazanfarian, R. Saghatchi, and D. Patil, "Implementation of Smoothed-Particle Hydrodynamics for non-linear Pennes' bioheat transfer equation," *Applied Mathematics and Computation*, vol 259, pp. 21-31, 2015.
- [21] P. K. Gupta, J. Singh, K. N. Rai, and S. Rai, "Solution of the heat transfer problem in tissues during hyperthermia by finite difference-decomposition method," *Applied Mathematics and Computation*, vol 219, pp. 6882-6892, 2013.
- [22] K. Khanafer, J. L. Bull, I. Pop, and R. Berguer, "Influence of pulsatile blood flow and heating scheme on the temperature distribution during hyperthermia treatment," *International Journal of Heat and Mass Transfer*, vol 50, pp. 4883-4890, 2007.
- [23] P. Yuan, "Numerical analysis of temperature and thermal dose response of biological tissues to thermal non-equilibrium during hyperthermia therapy," *Medical engineering & physics*, vol 30, pp. 135-143, 2008.
- [24] A. Jalali, M.-B. Ayani, and M. Baghban, "Simultaneous estimation of controllable parameters in a living tissue during thermal therapy," *Journal of thermal biology*, vol 45, pp. 37-42, 2014.
- [25] R. Jiwari, S. Pandit, and R. Mittal, "Numerical simulation of two-dimensional sine-Gordon solitons by differential quadrature method," *Computer Physics Communications*, vol 183, pp. 600-616, 2012.
- [26] C. W. Song, J. G. Rhee, and S. H. Levitt, "Blood flow in normal tissues and tumors during hyperthermia," *Journal of the National Cancer Institute*, vol 64, pp. 119-124, 1980.
- [27] S. R. Choudhuri, "On a thermoelastic three-phase-lag model," *Journal of Thermal Stresses*, vol 30, pp. 231-238, 2007.
- [28] D. Kumar, S. Singh, and K. Rai, "Analysis of classical Fourier, SPL and DPL heat transfer model in biological tissues in presence of metabolic and external heat source," *Heat and Mass Transfer*, vol 52, pp. 1089-1107, 2016.
- [29] D. Kumar and K. Rai, "A study on thermal damage during hyperthermia treatment based on DPL model for multilayer tissues using finite element Legendre wavelet Galerkin approach," *Journal of thermal biology*, vol 62, pp. 170-180, 2016.
- [30] D. Kumar, P. Kumar, and K. Rai, "Numerical solution of non-linear dual-phase-lag bioheat transfer equation within skin tissues," *Mathematical Biosciences*, vol 293, pp. 56-63, 2017.
- [31] D. Kumar and K. Rai, "Numerical simulation of time fractional dual-phase-lag model of heat transfer within skin tissue during thermal therapy," *Journal of Thermal Biology*, vol 67, pp. 49-58, 2017.
- [32] D. Kumar, S. Singh, N. Sharma, and K. Rai, "Verified non-linear DPL model with experimental data for analyzing heat transfer in tissue during thermal therapy," *International Journal of Thermal Sciences*, vol 133, pp. 320-329, 2018.
- [33] P. Kumar, D. Kumar, and K. Rai, "Numerical simulation of dual-phase-lag bioheat transfer model during thermal therapy," *Mathematical Biosciences*, vol 281, pp. 82-91, 2016.
- [34] P. Kumar, D. Kumar, and K. Rai, "A numerical study on dual-phase-lag model of bio-heat transfer during hyperthermia treatment," *Journal of thermal biology*, vol 49, pp. 98-105, 2015.
- [35] K.-C. Liu and H.-T. Chen, "Analysis for the dual-phase-lag bio-heat transfer during magnetic hyperthermia treatment," *International Journal of Heat and Mass Transfer*, vol 52, pp. 1185-1192, 2009.
- [36] R. Reis, F. Loureiro, and M. Lobosco, "A parallel 2D numerical simulation of tumor cells necrosis by local hyperthermia," in *Journal of Physics: Conference Series*, 2014, p. 012138.
- [37] S. K. Sharma and D. Kumar, "A study on non-linear DPL model for describing heat transfer in skin tissue during hyperthermia treatment," *entropy*, vol 22, p. 481, 2020.
- [38] H. Bagaria and D. Johnson, "Transient solution to the bioheat equation and optimization for magnetic fluid hyperthermia treatment," *International Journal of Hyperthermia*, vol 21, pp. 57-75, 2005.
- [39] P. K. Gupta, J. Singh, and K. Rai, "Numerical simulation for heat transfer in tissues during thermal therapy," *Journal of Thermal Biology*, vol 35, pp. 295-301, 2010.
- [40] Z.-W. Zhang, H. Wang, and Q.-H. Qin, "Method of fundamental solutions for nonlinear skin bioheat model," *Journal of Mechanics in Medicine and Biology*, vol 14, p. 1450060, 2014.
- [41] S. Singh, D. Kumar, and K. Rai, "Analytical solution of Fourier and non-Fourier heat transfer in longitudinal fin with internal heat generation and periodic boundary condition," *International Journal of Thermal Sciences*, vol 125, pp. 166-175, 2018.
- [42] M. Bhattacharya, "Finite-difference solutions of partial differential equations," *Communications in applied numerical methods*, vol 6, pp. 173-184, 1990.
- [43] J. C. Strikwerda, *Finite difference schemes and partial differential equations*: SIAM, 2004.
- [44] S. Guha and R. Srivastava, *Numerical Methods: For Engineering and Science*: Oxford University Press, 2010.
- [45] P. Bogacki and L. F. Shampine, "An efficient runge-kutta (4, 5) pair," *Computers & Mathematics with Applications*, vol 32, pp. 15-28, 1996.
- [46] J. H. Mathews and K. D. Fink, *Numerical methods using MATLAB* vol 4: Pearson prentice hall Upper Saddle River, NJ, 2004.
- [47] S. Mondal, A. Sur, and M. Kanoria, "Transient heating within skin tissue due to time-dependent thermal therapy in the context of memory dependent heat transport law," *Mechanics Based Design of Structures and Machines*, vol 49, pp. 271-285, 2021.